Quantum-confined biexcitons in $Si_{1-x}Ge_x$ grown on Si(001)

Kai Shum*
Department of Electrical Engineering, The City College of the City University of New York, New York, New York 10031

P. M. Mooney, L. P. Tilly,† and J. O. Chu
IBM Research Division, T. J. Watson Research Center, P.O. Box 218, Yorktown Heights, New York 10598

(Received 4 December 1996)

We report experimental evidence for the existence of three-dimensionally (3D) -confined biexcitons in a strain-relaxed $Si_{0.7}Ge_{0.3}$ layer grown on a stepwise graded buffer on Si(001) by ultrahigh vacuum chemical vapor deposition. A calculation of the photoluminescence line shape based on a simple model is found to be in good agreement with experiment. From this theoretical fit we deduce a binding energy of 1.55 meV for the 3D-confined biexcitons. This binding energy is larger than the reported value of 1.36 meV for a free biexciton in Si, indicating a quantum-confinement effect. [S0163-1829(97)07019-7]

Complex excitonic species such as multiple excitons bound to donors or acceptors, biexcitons, and polyexcitons in various semiconductor systems have been extensively studied because of their importance in the development of semiconductor physics[1] and for possible applications of these materials. Evidence of biexcitons in bulk Si was obtained by Gourley and Wolfe[2] and Thewalt and Rostworowski[3] from the infrared photoluminescence (PL) spectrum, and was later confirmed by Schmid[4] using the visible PL spectrum. Intrinsic polyexcitons were also observed in ultra-high-purity bulk Si by measuring the green PL spectrum over a range of sample temperatures.[5] Multiexciton complexes bound to shallow impurities in bulk Si (Ref. 4) and bulk SiGe alloys[6,7] have been carefully studied as well.

Although the optical properties of $Si_{1-x}Ge_x$ alloys have been extensively studied, no experimental evidence for the existence of intrinsic biexcitons in $Si_{1-x}Ge_x$ alloys has been reported, to our knowledge. In this paper, we report what we believe is the first experimental evidence for the existence of intrinsic three-dimensionally (3D) -confined biexcitons in strain-relaxed $Si_{0.7}Ge_{0.3}$ layers grown on a stepwise graded buffer on Si(100) by ultrahigh-vacuum chemical-vapor deposition (UHV/CVD).[8] A calculation of the PL line shape based on a simple model is found to be in good agreement with experiment. From this theoretical fit we deduce a binding energy of 1.55 meV for the 3D-confined biexcitons.

The high-sensitivity PL apparatus we used is as described previously,[9] except that the luminescence was collected by a lens instead of a parabolic mirror to enhance the collection efficiency further. Samples were excited by an Ar^+-ion laser at normal incidence by one of three lines: 458, 488, or 514.5 nm, with an excitation area of 1 mm^2. The samples were immersed in liquid or gaseous helium. The sample temperature was measured using a calibrated silicon diode, and could be varied continuously between 1.7 and 300 K. PL was analyzed by a computer-controlled Fourier-transform spectrometer, and detected by a liquid-nitrogen-cooled Ge detector. Measured PL spectra could be corrected for the systems spectral response using a blackbody radiator at a known temperature. However, the PL spectra presented here were not corrected since the system's spectral response is essentially flat in the spectral range of interest.

Data for two samples are reported here. Sample No. 1 is 3-μm-thick undoped $Si_{0.70}Ge_{0.30}$ layer which was grown on a stepwise graded buffer layer on a lightly boron-doped Si(001) substrate. A similar undoped sample, which shows the same spectral features as this one, has a background hole density of 6×10^{13} cm^{-3}, determined by a Hall-effect measurement at room temperature. Sample No. 2, also grown on a stepwise graded buffer layer, is a 1-μm-thick $Si_{0.68}Ge_{0.32}$ layer intentionally doped with 2×10^{16} cm^{-3} of boron, as determined from a capacitance-voltage measurement. The alloy composition and degree of strain relaxation of these SiGe layers were determined from double-crystal x-ray-diffraction measurements.[10] The average residual strain in sample No. 1 is 0.0003, and that in sample No. 2 is 0.0008.

Figure 1 shows the evolution of the PL spectra of sample No. 1 in the spectral region of the no-phonon-assisted excitonic emission taken at 2 K, as a function of the photoexcitation power density (P_{exc}) using the 514.5-nm laser line. The weak *D*-band emission originating from the dislocations in this sample was reported previously,[9] and will not be discussed here. Upon increasing the excitation power density, the PL spectra change remarkably. When P_{exc} is between 0.01 and 1 W/cm^2, the dominant emission is a narrow peak at 1.0457 eV; another broad peak at ~1.040 eV is dominant for P_{exc} from 1 to 50 W/cm^2. In contrast, the near-band-edge spectra of sample No. 2 consist of a single peak at 1.036 eV and its phonon replicas. This single peak was attributed to the no-phonon-assisted radiative annihilation of excitons bound to boron, $BE(B)^{np}$, in Ref. 9. Here we confirm that the 1.0457-eV emission in sample No. 1 is from 3D-confined excitons (CX), as was previously suggested.[9] We also show, however, that the ~1.040-eV peak is due to the annihilation of 3D-confined biexcitons (CX^2). This emission was previously attributed to excitons bound to phosphorous donors.[9]

There are two key experimental results which confirm the assignment of the 1.0457-eV emission to the CX. The first is the sample temperature dependence of the integrated PL intensity for both $BE(B)^{np}$and CX. Thermal activation energies of 2.1 meV for $BE(B)^{np}$ and 1.2 meV for CX was reported in

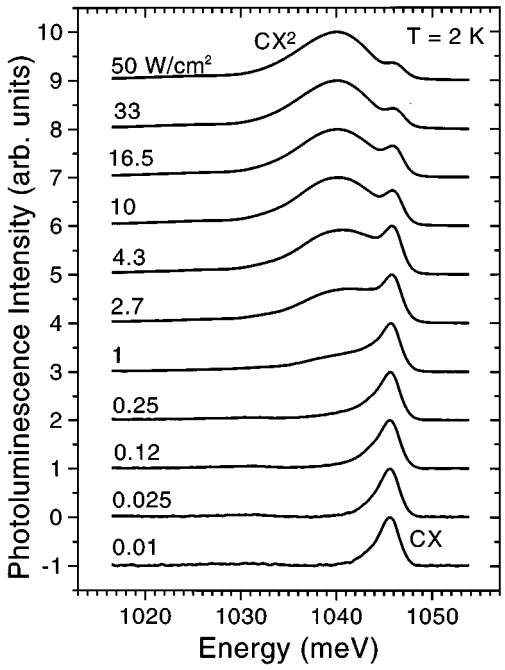

FIG. 1. PL spectra for sample No. 1 at 2 K using different excitation power densities. The peak centered at 1040 meV is due to confined biexciton emission. The peak at 1046 meV is due to confined exciton emission.

Ref. 9. These values are consistent with the assignment of $BE(B)^{np}$ and CX. The second set of data, shown in Fig. 2, is the sample temperature dependence of the PL peak energy for both $BE(B)^{np}$ and CX. The PL peak energy for $BE(B)^{np}$ follows the band-gap variation with temperature, as expected. The PL peak energy for CX shows a linear temperature dependence with a slope of 1 meV/K. This strong temperature dependence can only be interpreted using the model of a 3D-confined exciton. Confinement occurs because of fluctuations in alloy composition. The peak position would be expected to shift to lower energy as excitons which are thermally excited from shallower potential wells diffuse to deeper ones, i.e., excitons diffuse from regions of the alloy containing less Ge into regions having more Ge.

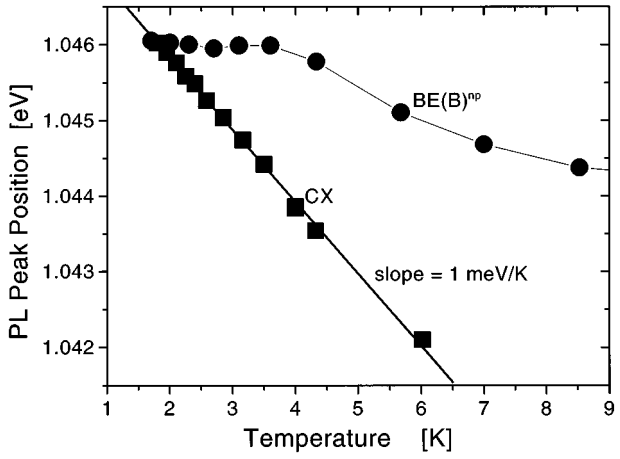

FIG. 2. Photoluminescence peak energy for 3D-confined excitons (CX) in sample No. 1 and for excitons bound to boron acceptors, $BE(B)^{np}$, in sample No. 2 plotted as a function of the sample temperature. The thick solid line is a linear fit to the CX data, giving a slope of 1 meV/K. The thin solid line is a guide for the eye.

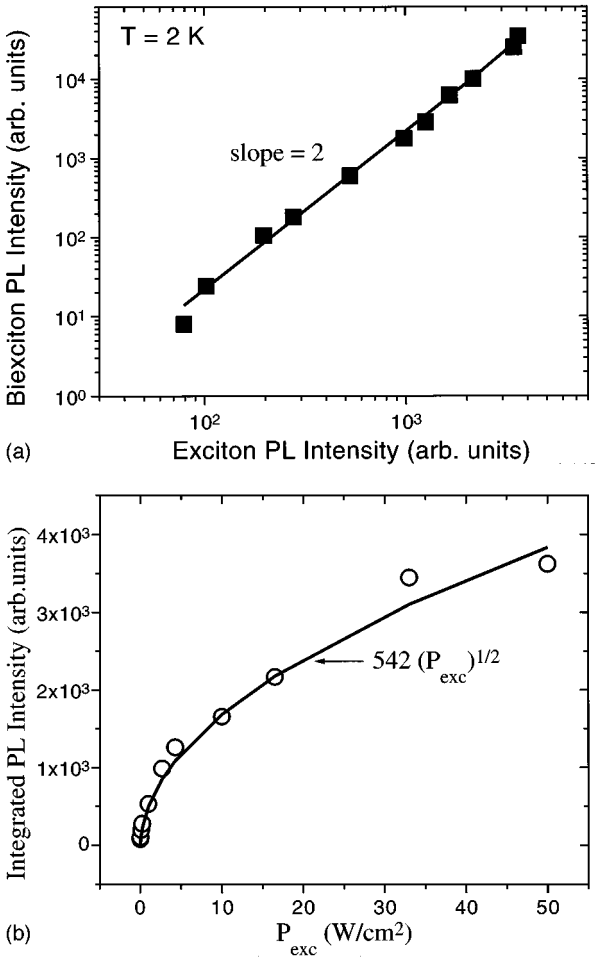

FIG. 3. (a) A log-log plot of the integrated PL intensity of the biexciton vs the integrated PL intensity of the exciton in sample No. 1. The solid line is a linear fit to the data giving a slope of 2. (b) The integrated PL intensity of the exciton emission in sample No. 1 as a function of the excitation power density. The solid curve is the theoretical curve calculated using the equation indicated on the plot.

With the firm assignment of the 1.0457-eV emission to the CX, the remaining task is to justify our assignment of the ~1.040-eV peak to CX^2, which is the primary goal of this paper. As analyzed by Gourley and Wolfe,[2] the fundamental relation of the chemical equilibrium condition for excitons and biexcitons confined in a potential well is the square law of equation

$$N_{cx2}/(N_{cx})^2 = N^*(T),$$

where $N^*(T)$ is a temperature dependent equilibrium constant, N_{cx2} is the total number of biexcitons, and N_{cx} is the total number of excitons. Assuming that the biexciton PL emission intensity I_{cx2} is proportional to N_{cx2}, and the exciton emission intensity I_{cx} is proportional to N_{cx}, then the relation $I_{cx} \propto (I_{cx})^2$ should hold at a given sample temperature. This fundamental square law is experimentally verified over three orders of magnitude for the biexciton PL intensity, as is shown in Fig. 3(a). This verification supports our assignment of CX^2. The strong increase of the CX^2 intensity at

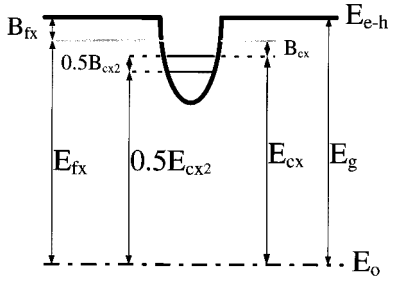

FIG. 4. Schematic energy-level diagram showing the various energies used to fit the exciton and biexciton line shapes. The potential well is shown by the thick solid line. Subscripts fx refer to free excitons, subscripts cx refer to confined excitons, and subscripts cx2 refer to confined biexcitons.

high power excitation density also rules out the earlier assignment,[9] of this peak to an exciton bound to a phosphorous impurity. Since the phosphorous concentration in these undoped samples is very low, we would expect the peak intensity of a phosphorous-bound exciton to saturate at high excitation power density.

Additional evidence for the validity of this assignment comes from the kinetic behavior. One can solve two coupled kinetic rate equations for a system of excitons and biexcitons by using an assumption, valid for an indirect-gap semiconductor, that the population of excitons and that of biexcitons are in thermal equilibrium.[2] Under steady-state conditions, $N_{cx} \propto (P_{exc})^{1/2}$. This relation is verified by our experimental data shown in Fig. 3(b), which shows that the intensity of the CX peak increases as the square root of P_{exc}. This $\frac{1}{2}$ power dependence of the exciton density on the excitation power density can occur for the case of a coupled biexciton-exciton system.

The strongest support for our CX^2 assignment comes, however, from the PL line-shape fitting. A schematic energy diagram of the potential well, i.e., at a Ge-rich region of the alloy, is depicted in Fig. 4 to illustrate the various energy levels used for the line-shape calculation. There are three excitonic energy levels (with zero kinetic energy) below the electron-hole pair energy (without Coulombic interaction), $E_{e\text{-}h}$, the free-exciton energy E_{fx}, the confined exciton energy E_{cx}, and the confined biexciton energy E_{cx2}. There are three binding energies, B_{fx}, B_{cx}, and B_{cx2}, for the free exciton, CX, and CX^2, respectively. Note that the symbol for each binding energy, which is a random variable associated with a Gaussian broadening function, represents a mean value. The biexciton binding energy is defined as

$$B_{cx2} = 2E_{cx} - E_{cx2}. \tag{1}$$

The following assumptions are made for fitting the CX^2 emission line shape: (1) phonons are not involved for the confined biexciton emission, (2) a Boltzmann distribution with an effective temperature T_{fx} is used for the free exciton system which is not in equilibrium with the confined excitons and biexcitons, (3) the density of states for the confined biexciton is energy independent, and (4) a Gaussian broadening function is used for B_{cx} and B_{cx2}. A radiative annihilation process of CX^2 obeys the energy conservation law

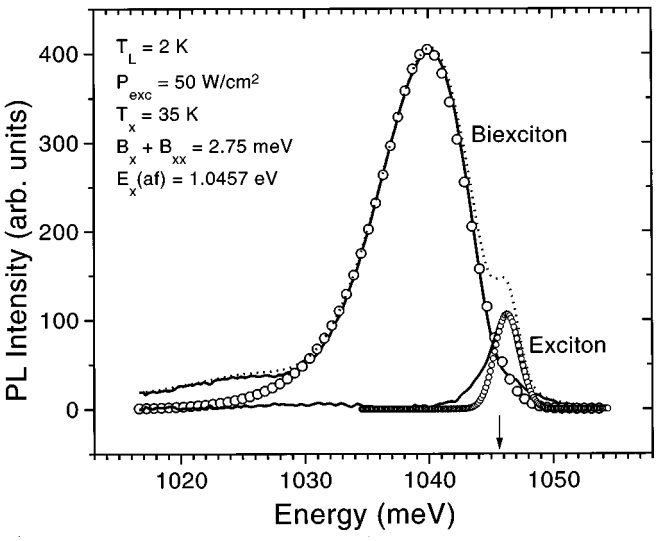

FIG. 5. Line-shape fitting for the spectrum of sample No. 1 taken at 2 K at a power excitation density of 50 W/cm^2. The dashed line shows the experimental data, which have been decomposed into the two spectra indicated by the solid curves. The open circles are the calculated spectra.

$$E_{cx2} = E_{fx} + E_k + \hbar\omega_{cx2}, \tag{2}$$

where E_k is the kinetic energy of the free exciton generated by the biexciton annihilation, and $\hbar\omega_{cx2}$ is the photon energy of the CX^2 emission. With the above assumptions and the energy conservation law, the line shape of CX^2 becomes[11,12]

$$I(\hbar\omega_{cx2}) \propto \int \exp[-(E_{cx} - y - \hbar\omega_{cx2})/K_B T] \times [E_{cx} - y - \hbar\omega_{cx2}]^{1/2} \Xi[E_{cx} - y - \hbar\omega_{cx2}] \times G(B, \sigma, y)\, dy, \tag{3}$$

where $G(B,\sigma,y)$ is a Gaussian broadening function with a mean value of $B = B_{cx} + B_{cx2}$ and variance σ, and Ξ is the Heaviside unit-step function. To accurately fit the experimental CX^2 line shape, we subtracted the CX contribution from each measured spectrum. The CX spectral line shape is assumed to be the same as the measured spectrum at the lowest excitation power density level, 0.01 W/cm^2, since at this low excitation level the CX^2 contribution to the spectrum is negligible.

Figure 5 shows our fitting results for the spectrum taken at 50 W/cm^2. The dashed curve is the measured spectrum which is the sum of two solid curves labeled as CX and CX^2. The open circles show the two calculated spectra. The CX spectrum was fit using a model line shape given by Gourley and Wolfe,[2] which has three parameters: the CX energy is $E_{cx} = 1.0457$ eV; the CX temperature is $T_{cx} = 2$ K, which is the same as the temperature of the crystal lattice; and the standard deviation of the Gaussian-broadening function is 0.93 meV. As can be seen from Fig. 4, the accuracy of the value of E_{cx} affects the accuracy in deducing the CX^2 binding energy from the line-shape fitting. The low-energy part of the CX spectrum did not fit well because of the residual CX^2 contribution.

The CX^2 spectrum was fit using Eq. (1). The fit is remarkably good. Note that the weak intensity near 1020 meV is due to the transverse acoustic-phonon replica which is not included in Eq. (1). Good modeling of the measured spectra was obtained over a wide range of the excitation levels from 1 to 50 W/cm^2. From this modeling, three important parameters were deduced: $B=2.75$ meV, $T_{fx}=35$ K, and $\sigma=2.4$ meV. This value for B is in excellent agreement with the thermal activation energy of 2.8 meV previously determined for this emission peak.[9] Since $B_{cx}=1.2$ meV was determined from the Arrhenius plot of the temperature dependence of the CX emission intensity,[9] the mean binding energy for the CX^2 can be obtained as $B_{cx2}=B-B_{cx}=1.55$ meV. This value for B_{cx2} is consistent with the thermodynamically determined binding energy of 1.53 meV reported for a biexciton confined in a strain-induced potential well in Si.[2] Since the binding energy for a free biexciton in bulk Si was determined to be 1.36 meV,[7] the increase of the binding energy by 0.19 meV (14%) for the 3D CX^2 in the SiGe alloy may be indicative of the quantum confinement effect. This quantum-confinement effect may also explain why such an intense no-phonon emission line was observed at low temperature in our samples, because the three-dimensional quantum confinement removes the momentum conservation requirement for optical transitions. The 14% gain in the biexciton binding energy can be compared to that in $GaAs/Al_xGa_{1-x}As$ quantum wells, where experimental values range from 25% to 100%, depending on the well width and the barrier height.[13]

The deduced effective free exciton temperature 35 K is well above the sample temperature. This is due to the expected ''recombination heating'' which has been observed for biexciton recombination processes in other semiconductor systems.[11,12] Keeping in mind that the data are collected within the biexciton recombination lifetime, the large deduced free exciton temperature may be dictated by the following three factors: (1) the initial excess energy left behind in the center-of-mass motion of the free exciton when a confined biexciton recombines; (2) the free exciton energy relaxation; and (3) the biexciton recombination lifetime, in which free excitons lose their kinetic energy to phonons. Further exploration of this requires additional time-resolved experiments and is beyond the scope of this paper.

In conclusion, we report the observation of three-dimensionally confined biexcitons in a relaxed $Si_{0.7}Ge_{0.3}$ alloy film grown on Si(001) by UHV/CVD. To our knowledge, this is the first report on confined biexcitons in ''bulk'' SiGe alloys. The binding energy of the confined biexciton was determined to be 1.55 meV. The enhancement of the confined biexciton binding energy is indicative of a quantum-confinement effect.

We thank K. Ismail for the Hall effect measurement, L.P.T. gratefully acknowledges financial support from the Swedish Research Council for Engineering Sciences. K.S. was partially supported by a grant (No. F49620-93-1-0619) from AFOSR. K.S. and L.P.T. would like to thank B.S. Meyerson and A. Grill for their support while at IBM. This work was done while on a special leave at IBM T. J. Watson Research Center.

*Electronic address: shum@ee.mail.engr.ccny.cuny.edu
†Present address: Ericsson Components AB, Kista-Stockholm, Sweden.

[1] M. A. Lampert, Phys. Rev. Lett. **1**, 450 (1958).
[2] P. L. Gourley and J. P. Wolfe, Phys. Rev. Lett. **40**, 526 (1978); Phys. Rev. B **20**, 3319 (1979).
[3] M. L. W. Thewalt and J. A. Rostworowski, Solid State Commun. **25**, 991 (1978).
[4] W. Schmid, Phys. Rev. Lett. **45**, 1726 (1980).
[5] A. G. Steele, W. G. McMullan, and M. L. W. Thewalt, Phys. Rev. Lett. **59**, 2899 (1987).
[6] G. S. Mitchard and T. C. McGill, Phys. Rev. B **25**, 5351 (1982).
[7] J. Weber and M. I. Alonso, Phys. Rev. B **40**, 5683 (1989).
[8] B. S. Meyerson, Appl. Phys. Lett. **48**, 797 (1986).
[9] L. P. Tilly, P. M. Mooney, J. O. Chu, and F. K. LeGoues, Appl. Phys. Lett. **67**, 2488 (1995).
[10] P. M. Mooney, F. K. LeGoues, J. O. Chu, and S. F. Nelson, Appl. Phys. Lett. **62**, 3464 (1993).
[11] R. T. Phillips, D. J. Lovering, G. J. Denton, and G. W. Smith, Phys. Rev. B **45**, 4308 (1992).
[12] D. Birkedal, J. Singh, V. G. Lyssenko, J. Erland, and J. M. Hvam, Phys. Rev. Lett. **76**, 672 (1996).
[13] D. C. Reynolds, K. K. Bajaj, C. E. Stutz, R. L. Jones, W. M. Theis, P. W. Yu, and K. R. Evans, Phys. Rev. B **40**, 3330 (1989).